

AD-A129 527

PULSED CHEMICAL LASER WITH VARIABLE-PULSE-LENGTH
ELECTRON-BEAM INITIATION..(U) AEROSPACE CORP EL SEGUNDO
CA AEROPHYSICS LAB S T AMIMOTO ET AL. 25 APR 83

1/1

UNCLASSIFIED

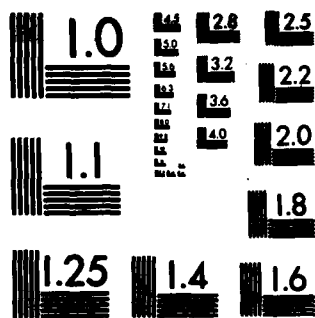
TR-0083(3606)-1 SD-TR-83-28

F/G 20/5

NL



END
DATE
FILMED
7 83
DTIC



MICROCOPY RESOLUTION TEST CHART
NATIONAL BUREAU OF STANDARDS-1963-A

ADA 1 29527

DTC FILE COPY

Prepared for
AIR FORCE WEAPONS LABORATORY
Kirtland Air Force Base, N. Mex. 87117

SPACE DIVISION
AIR FORCE SYSTEMS COMMAND
Los Angeles Air Force Station
P.O. Box 92960, Worldway Postal Center
Los Angeles, Calif. 90009

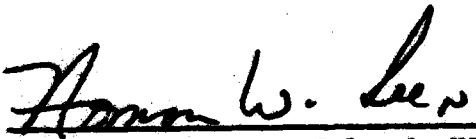
83 06 21 069

This report was submitted by The Aerospace Corporation, El Segundo, CA 90245, under Contract No. F04701-82-C-0083 with the Space Division, Deputy for Technology, P.O. Box 92960, Worldway Postal Center, Los Angeles, CA 90009. It was reviewed and approved for The Aerospace Corporation by W. P. Thompson, Jr., Director, Aerophysics Laboratory. 1st Lt Steven G. Webb was the Air Force project officer.

This report has been reviewed by the Public Affairs Office (PAS) and is releasable to the National Technical Information Service (NTIS). At NTIS, it will be available to the general public, including foreign nationals.

This technical report has been reviewed and is approved for publication. Publication of this report does not constitute Air Force approval of the report's findings or conclusions. It is published only for the exchange and stimulation of ideas.


Steven G. Webb, 1st Lt, USAF
Project Officer


Norman W. Lee, Jr., Colonel, USAF
Commander, Det 1, AFSTC

CONTENTS

PULSED CHEMICAL LASER WITH VARIABLE-PULSE-LENGTH
ELECTRON-BEAM INITIATION AND MAGNETIC CONFINEMENT..... 3

REFERENCES..... 13

FIGURES

1. Electron-Beam Accelerator Equivalent Circuit..... 5

2. Apparatus Cross Section..... 6

3. Laser Energy Density Versus Pulse Length and Charge Fluence..... 9

4. Typical Data for Long-Pulse Electron-Beam Initiation..... 10

5. Laser Specific Energy Versus Scaling Parameter..... 11



Accession For	
DTIC GRA&I	<input checked="" type="checkbox"/>
DTIC TAB	<input type="checkbox"/>
Unannounced	<input type="checkbox"/>
Justification	
By	
Distribution/	
Availability Codes	
Dist	Avail at /or Special
A	

PULSED CHEMICAL LASER WITH VARIABLE-PULSE-LENGTH
ELECTRON-BEAM INITIATION AND MAGNETIC CONFINEMENT

Electron-beam initiation of pulsed HF chain-reaction lasers has been studied by a number of investigators.¹⁻¹⁰ Interest in the use of electron beams has been motivated by their potential for excitation of large volumes and by the possibility for extraction of laser energies in excess of the electrical energy expended for initiation. In a recent demonstration,¹ longitudinal initiation by a 7-kJ, 70-ns electron beam produced a 4.2-kJ HF laser output of 20-ns (FWHM) duration; the corresponding intrinsic electrical efficiency (laser output/deposited electron-beam energy) in this work is 180%. Mangano et al.,² operating at much lower current densities (20 A/cm²) and longer electron-beam pulse durations (0.2 μ s), reported intrinsic electrical efficiencies as high as 875% at laser output energy densities of 51 J/liter. By comparison of the experimental rate of F₂ disappearance with theoretical pulsed HF laser code predictions,³ we recently reported the efficient production of chain carriers by an electron beam operating at relatively low current densities.⁴ The present investigation extends the work of earlier investigators to longer electron-beam pulse lengths and lower current densities. We seek to establish scale size limitations for transversely pumped electron-beam-initiated chemical lasers and to increase the permissible limit of laser pulse repetition frequency (as constrained by anode foil heating). We also report the first data on the effect of a confining transverse magnetic field¹¹ on pulsed HF laser performance. The purpose of the confining B-field is to overwhelm steering effects of self-fields accompanying electron-beam generation and to capture foil- and gas-scattered electrons in Larmor spirals to promote efficient and uniform transport of electrons across the active laser medium.

An existing pulsed electron accelerator system⁶ was modified for the generation of long-duration electron-beam pulses and confinement by strong magnetic fields. The electron gun was driven by a pulse-forming network comprised of a four-stage Marx generator, a low impedance coaxial water line that

was operated as a peaking capacitor and a high-voltage output switch (Fig. 1). Use of the "peaking-capacitor mode" of operation permitted the investigation of the effect of cathode risetime on emission uniformity and laser performance. Several cold-cathode emitter concepts were tested for their compatibility with strong confining magnetic fields.¹² The desired current densities and beam uniformity were achieved by means of thermally conditioned carbon felt emitters.¹³ A 10 x 100 cm section of felt was held by a stainless steel cathode structure that was slotted to minimize magnetic steering of electrons into the window-holder webbing (Fig. 2). The electron window consisted of a pair of stainless steel rib supports of 82% transmission that clamped between them a 76- μ m film of aluminized Kapton. On the vacuum side of the electron window was located one element of a Helmholtz coil through which an electron beam of 5 x 100 cm cross section was transmitted. A second coil element was positioned at the rear of the laser chamber to produce a nearly uniform confining B-field within the volume of the active laser medium. With this Helmholtz coil arrangement, magnetic fields of up to 1.3 kG were produced. At the exit of the anode window, a uniform ($\pm 10\%$) variable current-density electron beam of approximately 175 kV was transmitted across the laser cavity. Nominal current densities of 7 and 12 A/cm² were produced using anode-cathode spacings of 5.0 and 3.8 cm, respectively. A low-inductance crowbar switch located at the output of the Marx generator was fired from a "bootstrap" trigger to generate continuously variable electron-beam pulse lengths in the range 0.2 to 1.2 μ s. Routine diagnostic measurements of Marx current and voltage, total diode current, electron-beam current density, and diode accelerating voltage were obtained during each laser test.

Laser gas flows were established by conventional methods.⁶ Commercial purity O₂, F₂, and He were premixed and flowed through a regulator to a mixer where they were injected through a calibrated sonic orifice. Metered flows of the remaining commercial-purity gases (D₂, H₂, NF₃, Ar, SF₆, and/or additional He) were introduced into the mixer through another sonic orifice. Typically, 3 to 4 min were required to raise the laser chamber to an operating pressure of 800 Torr. Before and immediately following initiation, nominal mixture composition has been verified in previous studies by an in situ measurement of

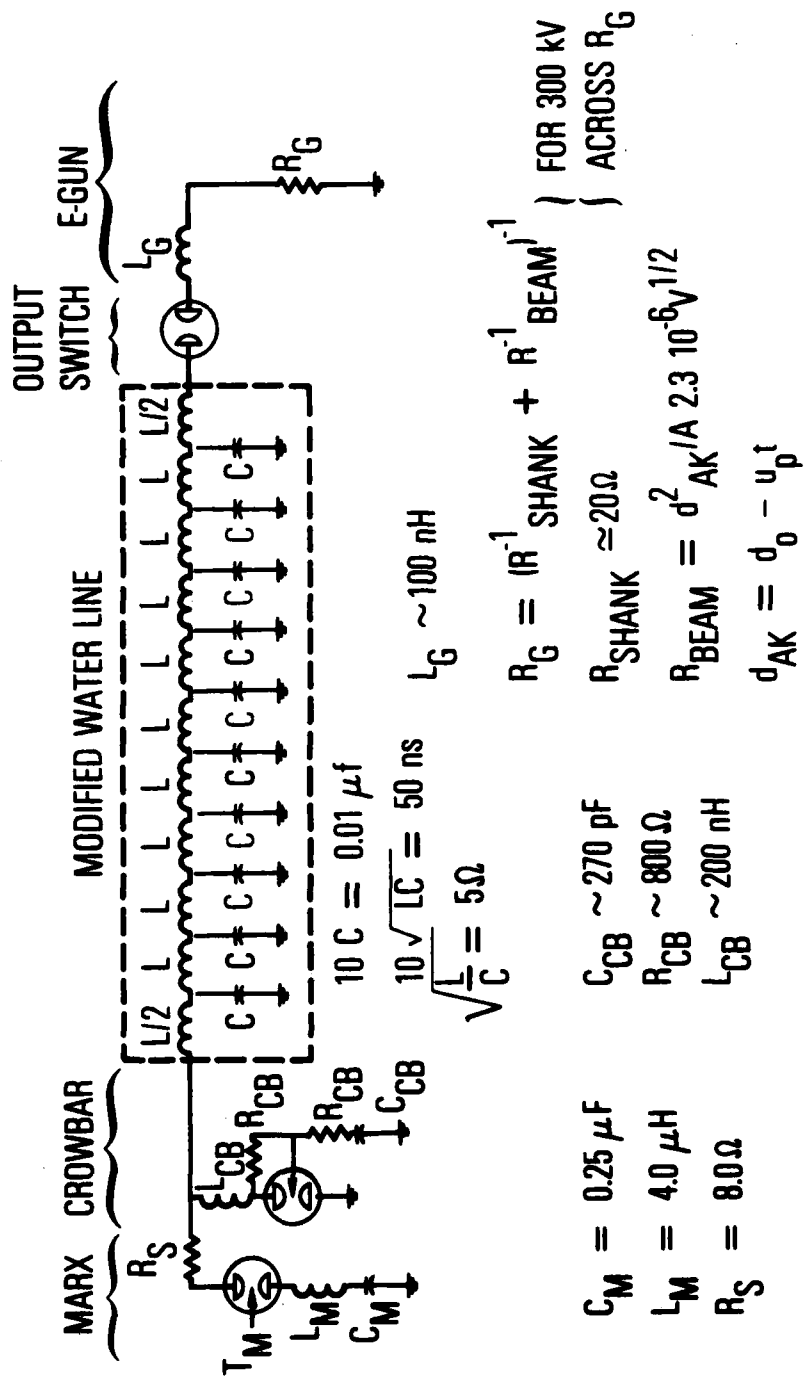


Fig. 1. Electron-Beam Accelerator Equivalent Circuit. The Marx bank is represented by a single capacitor, switch, and inductor at the left side of the figure. The water line, shown as a distributed transmission line, is charged through a series resistor, R_S . With adjustment of the peaking capacitor in the output switch, the water line is operated in the peaking capacitor mode, allowing fast risetimes to be obtained and testing of various cold cathode concepts. The electron-gun impedance is modeled as a nonlinear time varying impedance and shank loss and is represented in this figure as R_G .

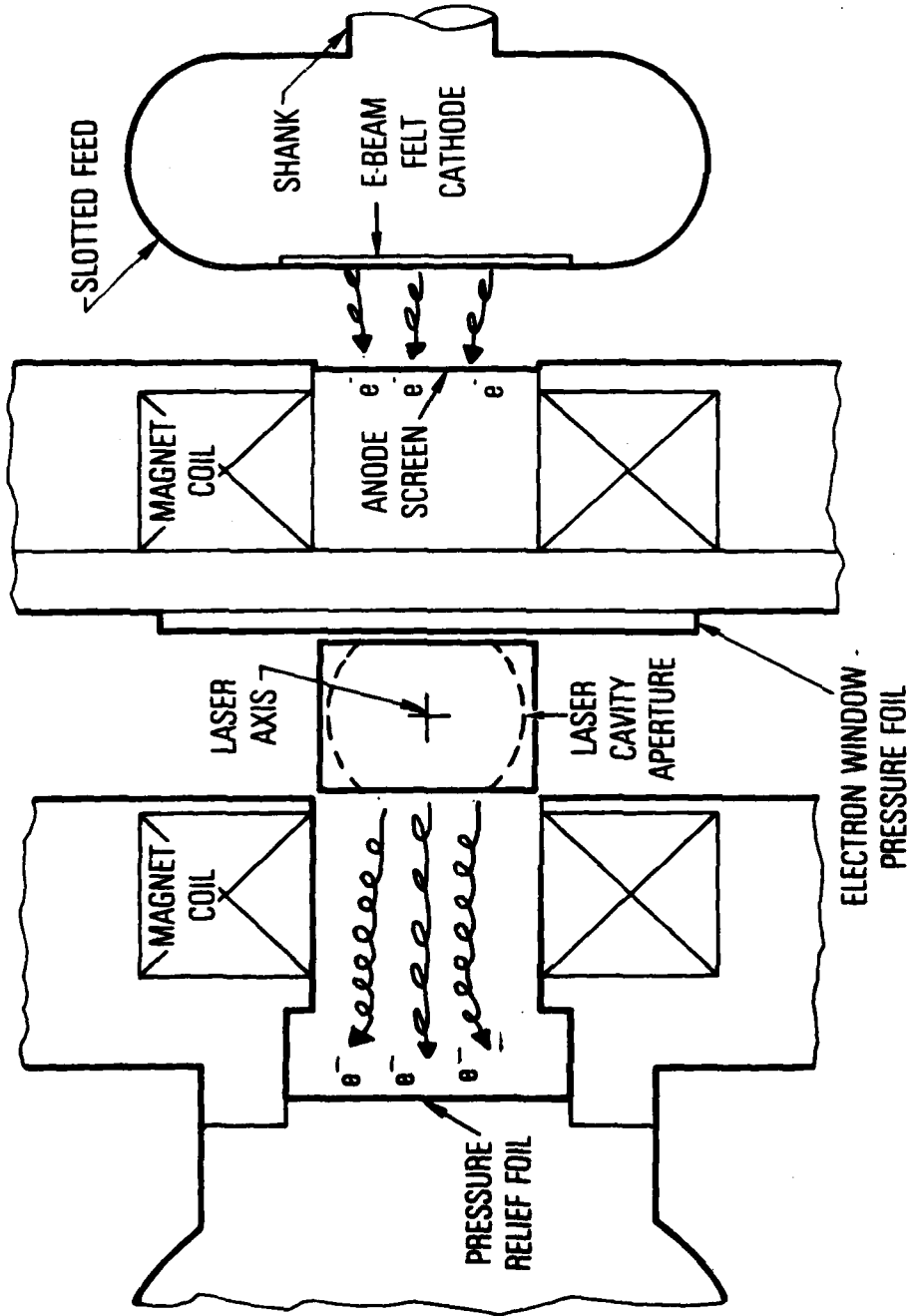


Fig. 2. Apparatus Cross Section. A cross section of experimental apparatus is shown. Electrons originate at the carbon felt cathode that is mounted on a slotted feed. They are accelerated toward the anode and confined by the magnetic field produced by a pair of Helmholtz coils. The electrons pass through the electron foil window and enter the laser cavity. The cross section of the laser aperture is 20 cm^2 , whereas the active length of the cavity is $\sim 1 \text{ m}$. Following initiation, a set of aluminum rupture foils is ruptured, allowing the initiated laser mixture to expand into a dump tank located on the far left of the figure.

F_2 concentration employing an ultraviolet absorption technique.⁴ HF probe laser measurements performed during an earlier unpublished study indicated that $HF/F_2 < 5 \times 10^{-3}$; hence, prereaction is believed to be unimportant for the data presented herein.

Laser performance was investigated using both stable and unstable optical resonators. Three confocal unstable resonators of magnification 1.3, 1.8, and 2.8 were employed. Cavity elements consisted of highly polished oxygen-free, high conductivity uncoated copper mirrors of high optical figure. The nominal Fresnel number of the unstable resonators was 160. A 2.5-m stable resonator was formed by a gold-coated concave spherical mirror with a radius of 4.5 m and either a silicon or sapphire flat output coupler. Laser windows were uncoated 1.25-cm thick CaF_2 crystals that were tilted with respect to the optical axis. The optical axis of the resonator was centered on the 5 x 5 x 100 cm volume being excited by the transverse electron beam. The clear apertures of the cavity elements limited the optical extraction volume to 2 liters, as verified by near-field laser burn patterns.

Laser pulse energy was measured with ballistic thermopiles of 4- and 9-cm entrance apertures. Nearly all of the laser pulse energy was directed into the 9-cm calorimeter on every test. A beam splitter at nearly normal incidence to the laser beam diverted about 3% of the total pulse energy into the 4-cm calorimeter. The two calorimeters tracked one another, except at the highest energy condition, where slight self-shielding of the large calorimeter by a laser-supported combustion wave is believed to have occurred. Emission time history of the laser was monitored with an Au:Ge detector.

The trends of laser performance with several parameters have been studied. Using a tantalum blade emitter cathode in the absence of a confining magnetic field, laser output was measured as a function of electron-beam charge fluence and electron-beam pulse duration. Laser mixtures containing 20% F_2 : 8 H_2 : 25 SF_6 : 43.5 He : 3.5 O_2 by volume were examined in this set of experiments. Electron-beam pulse widths were varied between 0.2 and 1.2 μs , and nominal current densities were 8 A/cm^2 . At a charge fluence of 10 $\mu C/cm^2$, a laser

output of 46 J/liter was measured (Fig. 3). These experiments were performed without benefit of a confining magnetic field.

The same mixtures and electron-beam parameters used in the preceding paragraph were investigated with a carbon felt cathode in place of the blade emitter. With no B-field present, carbon-felt and blade-emitter laser performance were comparable. When a 1.3 kG field was imposed, laser output increased 100 to 200% over the zero field performance, depending upon the value of electron-beam current density and charge fluence (Fig. 3). The major effects of the confining B-field are to overwhelm steering effects of self-fields accompanying electron-beam generation, to capture foil and gas-scattered electrons in Larmor spirals, and to slightly focus the electron beam into the clear aperture defined by the anode magnet coil holder. At an electron-beam pulse duration of 0.6 μs ($3.5 \mu\text{C}/\text{cm}^2$), laser outputs of 65 J/liter were measured, and laser pulse lengths of 0.8 μs FWHM were observed (Fig. 4). For electron-beam pulse lengths of 0.6 μs or less, laser energy density was found to vary with the square root of initiation strength (electron-beam charge fluence), as anticipated on theoretical grounds (Fig. 5).¹⁴ For electron-beam pulse lengths between 0.6 and 1.2 μs , no further increase in laser output was observed. This effect of saturation in performance of high-energy density mixtures with increasing initiator pulse length has not previously been reported.

In previous unpublished experiments, we obtained 65 J/liter HF output with a 70-ns 400-keV electron beam and incident charge fluences of $3.5 \mu\text{C}/\text{cm}^2$. Comprehensive rotational-nonequilibrium chemical laser modeling³ has predicted a 20% degradation in laser output (due to ion deactivation and slower rate of initiation) with μs -duration electron-beam initiation compared with 70-ns initiation. Experimental results at $3.5 \mu\text{C}/\text{cm}^2$ showed, however, the same laser output (65 J/liter) with a 0.6- μs electron beam as with a 70-ns electron beam, and a somewhat longer laser pulse length¹⁵ with long duration electron-beam initiation (0.8 versus 0.5 μs FWHM at 70 ns). These results suggest the possibility of large volume excitation by the present initiator approach.

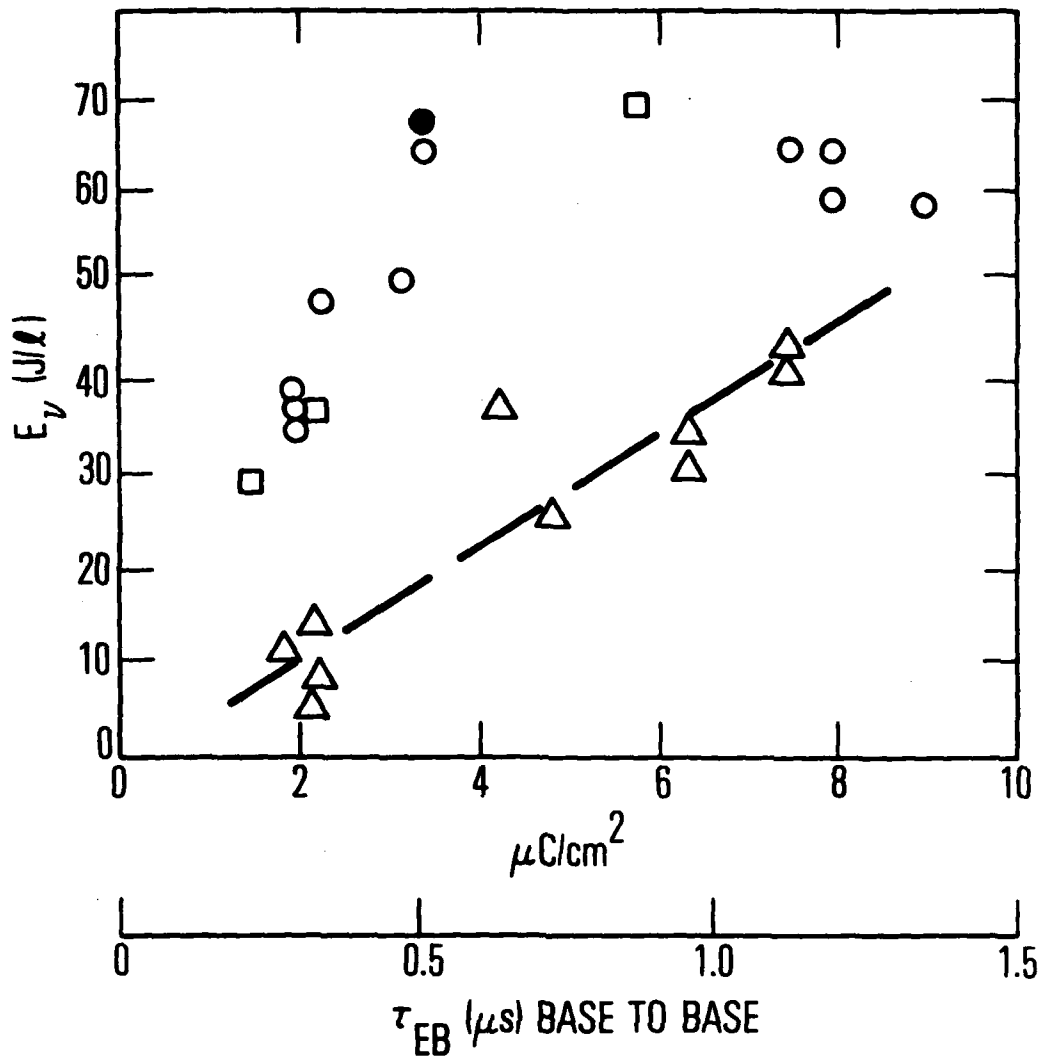
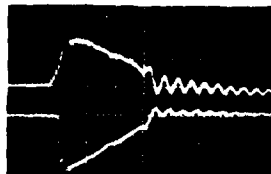


Fig. 3. Laser Energy Density Versus Pulse Length and Charge Fluence. Energy output from 20 F₂; 8 H₂; 25 SF₆; 44 He; 3 O₂ mixtures at 800 Torr pressure is plotted as a function of charge fluence delivered at the electron window. The zero B-field data (Δ) were obtained with a tantalum blade cathode. The single point (\bullet) was obtained using a 70 ns electron-beam pulse. Carbon felt data employing stable (\circ) and unstable (\square) resonators in the presence of a 1.3 kG field illustrate the advantage of a strong confining magnetic field; for these data, laser performance reaches a plateau near 3.5 $\mu\text{C}/\text{cm}^2$. No significant difference in performance is observed between short (70 ns) and long (0.6 μs) pulse electron-beam initiation at 3.5 $\mu\text{C}/\text{cm}^2$.

V_{CATHODE}
160 kV/DIV
 V_{TUBE}
130 kV/DIV



IR
 $\frac{3.9 \text{ MW/cm}^2}{\text{DIV}}$



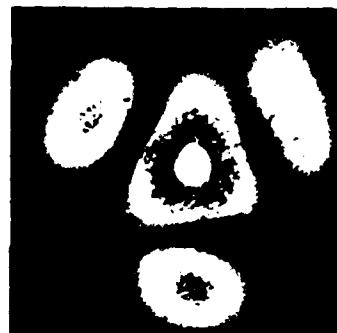
ROGOWSKI STRIP
6.4 ka/DIV



FARADAY CUP
 $\frac{4 \mu\text{a/cm}^2}{\text{DIV}}$

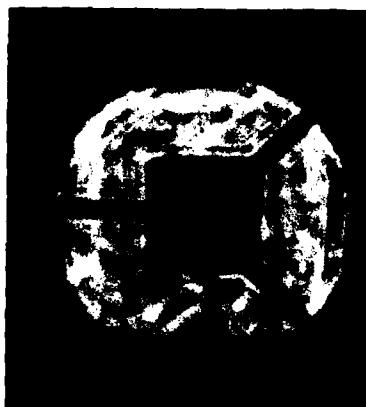


0.5 $\mu\text{s/DIV}$



FAR-FIELD BURN

0.40 mm



NEAR-FIELD BURN

5 cm

Fig. 4. Typical Data for Long-Pulse Electron-Beam Initiation. Data are shown for a 20 F₂: 8 H₂: 25 SF₆: 3.5 O₂: 43.5 He mixture at 800 Torr for the case of a 1.3-kG confining magnetic field. A carbon felt cathode was used for generation of these data. Oscillograms are shown for Marx voltage and diode accelerating voltage, laser irradiance, total gun current, and current density at the exit of the gain region. The electron-beam pulse length is 1.2 μs (base-to-base). Laser output is 65 J/liter with a 0.8 μs (FWHM) laser pulsewidth. The near-field burn pattern shows that the laser beam possesses a high degree of coherence. The fact that most of the laser energy is contained within the first Airey disk in the far-field burn is evidence of good beam quality.

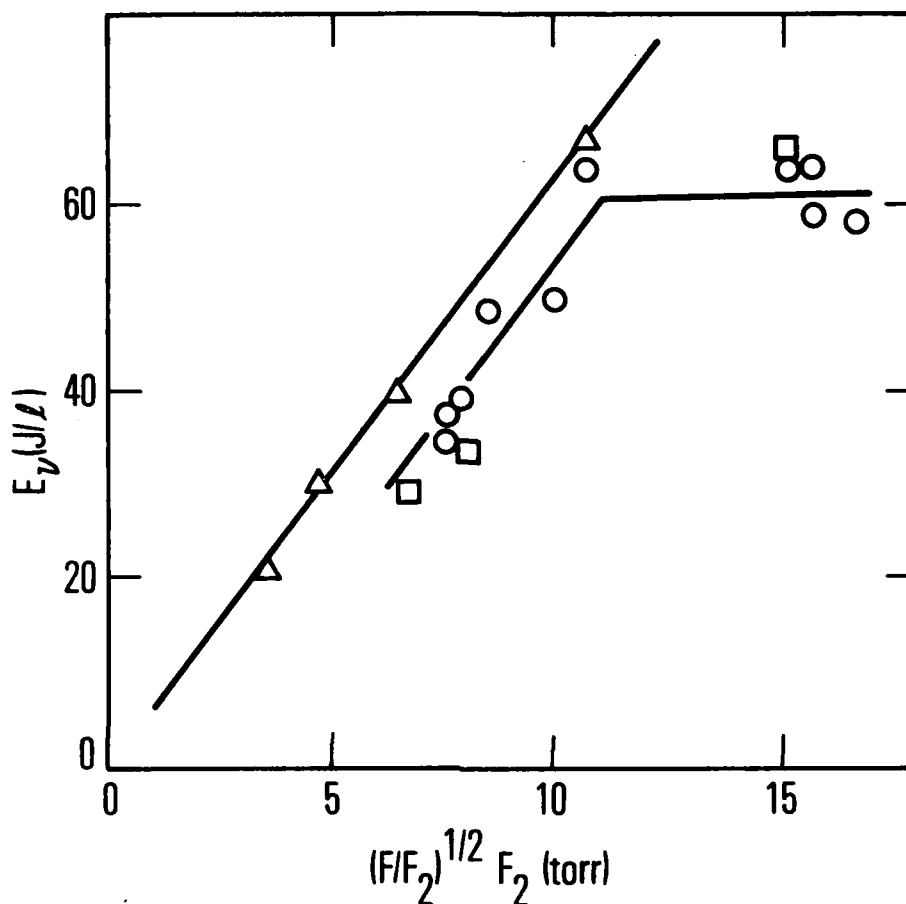


Fig. 5. Laser Specific Energy Versus Scaling Parameter. HF performance is plotted as a function of the scaling parameter $(F/F_2)^{1/2} F_2$, derived in Ref. 14. Initiation level F/F_2 is estimated for various mixtures by scaling previously measured initiation levels⁴ with measured charge fluence and mixture stopping power.¹⁶ The results for 70 ns electron-beam initiation (Δ) were obtained without magnetic confinement using an incident electron-beam charge fluence of $3.5 \mu\text{C}/\text{cm}^2$; the extent of laser mixture dilution was varied in order to obtain the data points shown. The data for 1.3 kG B-field using unstable (\square) and stable (\circ) resonators indicate a slightly lower performance than the 70 ns data; these data also exhibit saturation near $(F/F_2)^{1/2} F_2 = 10$ Torr.

The performance of unstable resonators was also investigated. No penalty in energy performance was observed with the substitution of an unstable resonator for a stable resonator. Moreover, near- and far-field burn patterns on witness plates indicated evidence of good beam quality as had been anticipated from earlier unpublished measurements of optical homogeneity of the medium (Fig. 4).

The largest HF laser output, 158 J (79 J/liter), was obtained with an electrical input incident on the extraction volume of about 350 J; chemical efficiency relative to the initial H₂ content was 4.6%. The electrical efficiency for conversion of total incident energy to laser output energy was, therefore, 45%. Based on the stopping power data of Ref. 16, the intrinsic electrical efficiency for this case is calculated to be 380%. High overall electrical efficiencies well in excess of 100% appear possible for the subject laser device when the dimension along the axis of electron-beam propagation is made comparable to the range of the electron beam.

The experimental results demonstrate that attractive HF chain laser performance (79 J/liter) and good beam quality can be achieved using long-duration, low-current density electron-beam initiation and magnetic confinement. The data imply that large-volume excitation of pulsed-HF chain lasers is feasible and should be compatible with high laser energy densities and large overall electrical efficiencies.

REFERENCES

1. R. A. Gerber and E. L. Patterson, *J. Appl. Phys.* 47, 3524 (1976).
2. J. A. Mangano, R. L. Limpacher, J. D. Daugherty, and F. Russell, *Appl. Phys. Lett.* 27, 293 (1975).
3. J. J. T. Hough, *Appl. Opt.* 16, 2297 (1977); also, *Opt. Lett.* 3, 223 (1978).
4. J. S. Whittier, M. L. Lundquist, A. Ching, G. Thornton, and R. Hofland, *J. Appl. Phys.* 47, 3542 (1976).
5. V. F. Zharov, V. K. Malinovskii, Yu. S. Neganov, and G. M. Chumak, *JETP Lett.* 16, 154 (1972).
6. R. Hofland, A. Ching, M. L. Lundquist, and J. S. Whittier, *IEEE J. Quantum Electron.* QE-10, 781 (1974); also, *J. Appl. Phys.* 47, 4543 (1976).
7. E. L. Patterson, R. A. Gerber, and L. S. Blair, *J. Appl. Phys.* 45, 1822 (1974).
8. R. Aprahamian, J. H. S. Wang, J. A. Betts, R. W. Barth, *Appl. Phys. Lett.* 24, 239 (1974).
9. V. I. Igoshin, V. Yu. Nikitin, and A. N. Oraevskii, *Sov. J. Quantum Electron.* 6, 1132 (1976).
10. A. S. Bashkin, A. F. Konoshenko, A. N. Oraevskii, V. N. Tomashov, and N. N. Yuryshv, *Sov. J. Quantum Electron.* 8, 922 (1979).
11. C. Duzy and J. Boness, *IEEE J. Quantum Electron.* QE-16, 640 (1980).
12. G. Loda, Systems, Science, and Software, private communication.
13. J. H. Tillotson and J. Shannon, "Efficient Electron Beam Generation and Transmission," MLR-783, Maxwell Laboratories (February 1978).
14. H. Mirels, R. Hofland, and J. S. Whittier, *J. Appl. Phys.* 50, 6660 (1979).
15. H. Mirels, "The Effect of Initiator Duration on Pulsed Chemical Laser Performance," to appear *J. Appl. Phys.*
16. L. Pages, E. Bertel, H. Joffre, and L. Sklavenitis, *Atomic Data* 4, 1-127 (1972).

LABORATORY OPERATIONS

The Laboratory Operations of The Aerospace Corporation is conducting experimental and theoretical investigations necessary for the evaluation and application of scientific advances, to new military space systems. Versatility and flexibility have been developed to a high degree by the laboratory personnel in dealing with the many problems encountered in the nation's rapidly developing space systems. Expertise in the latest scientific developments is vital to the accomplishment of tasks related to these problems. The laboratories that contribute to this research are:

Aerophysics Laboratory: Launch vehicle and reentry aerodynamics and heat transfer, propulsion chemistry and fluid mechanics, structural mechanics, flight dynamics; high-temperature thermomechanics, gas kinetics and radiation; research in environmental chemistry and contamination; cw and pulsed chemical laser development including chemical kinetics, spectroscopy, optical resonators and beam pointing, atmospheric propagation, laser effects and countermeasures.

Chemistry and Physics Laboratory: Atmospheric chemical reactions, atmospheric optics, light scattering, state-specific chemical reactions and radiation transport in rocket plumes, applied laser spectroscopy, laser chemistry, battery electrochemistry, space vacuum and radiation effects on materials, lubrication and surface phenomena, thermionic emission, photosensitive materials and detectors, atomic frequency standards, and bioenvironmental research and monitoring.

Electronics Research Laboratory: Microelectronics, GaAs low-noise and power devices, semiconductor lasers, electromagnetic and optical propagation phenomena, quantum electronics, laser communications, lidar, and electro-optics; communication sciences, applied electronics, semiconductor crystal and device physics, radiometric imaging; millimeter-wave and microwave technology.

Information Sciences Research Office: Program verification, program translation, performance-sensitive system design, distributed architectures for spaceborne computers, fault-tolerant computer systems, artificial intelligence, and microelectronics applications.

Materials Sciences Laboratory: Development of new materials: metal matrix composites, polymers, and new forms of carbon; component failure analysis and reliability; fracture mechanics and stress corrosion; evaluation of materials in space environment; materials performance in space transportation systems; analysis of systems vulnerability and survivability in enemy-induced environments.

Space Sciences Laboratory: Atmospheric and ionospheric physics, radiation from the atmosphere, density and composition of the upper atmosphere, aurorae and airglow; magnetospheric physics, cosmic rays, generation and propagation of plasma waves in the magnetosphere; solar physics, infrared astronomy; the effects of nuclear explosions, magnetic storms, and solar activity on the earth's atmosphere, ionosphere, and magnetosphere; the effects of optical, electromagnetic, and particulate radiations in space on space systems.